# The Mach-Zehnder Interferometer Based on Silicon Oxides for Label Free Detection of C-reactive Protein (CRP)

### Jongin Hong<sup>1</sup>, Daesung Yoon<sup>2</sup> & Tae Song Kim<sup>3</sup>

<sup>1</sup>Department of Chemistry, Imperial College London, South Kensington Campus, London SW7 2AZ, UK <sup>2</sup>Department of Biomedical Engineering, Yonsei University, 234 Maeji-ri, Heungup-myeon, Wonju-si, Gangwon-do 220-710, Korea <sup>3</sup>Korea Institute of Science and Technology, 39-1 Hawolgok-dong, Seongbuk-gu, Seoul 136-791, Korea

Correspondence and requests for materials should be addressed to J. Hong (hong.jongin@gmail.com)

Accepted 12 January 2009

# Abstract

The C-reactive protein (CRP) is a very important inflammation biomarker and a major predictor of cardiovascular disease (CVD) in human. We demonstrated here on a new approach to determine the binding of label free CRP to monoclonal anti-CRP using the Mach-Zehnder interferometer based on silicon oxides with the detection limit of 1 ng/mL or even less at the operating wavelength of 1,550 nm. The building block, single-mode waveguide of total internal reflection, was precisely designed using a finite element method (FEM) and so we suggested the guideline of microfabrication to achieve it. We also firstly introduced the calixcrown self-assembled monolayers (SAMs), which guaranteed the activity of capture proteins and the correct orientation, to immobilize the monoclonal anti-CRP on PECVD silicon oxides into the biosensors based on the interaction of the evanescent field of the guided light with the surrounding environment.

**Keywords:** C-reactive protein, Mach-Zehnder interferometer, Biosensor, Finite element method, Silicon oxide

# Introduction

For the last decade, immunosensors have been developed to transform efficiently a biological reaction into a measurable signal for biological process, healthcare, drug discovery, medical diagnostics, environmental monitoring, food industry and military defense<sup>1-4</sup>. Among several transduction methods, optical transducers offer more attractive characteristics including

high sensitivity and immunity to electromagnetic interference. In the optical transducers, biological reaction produces a change in the vicinity of a light path and then this variation induces a change in the propagation properties of light. Initiated by the pioneering work of Tiefenthaler and Lukosz<sup>5</sup>, an integrated optics has been an impetus to develop compact sensing devices with high sensitivity, fast response time and real-time monitoring. The integrated optic biosensor utilizes the evanescent field to detect biological events at the waveguide surface and it has opened the possibility of miniaturization, robustness and mass production<sup>6-9</sup>. Importantly, a Mach-Zehnder interferometer (MZI) sensor has been a promising candidate because of extremely high sensitivity and an internal reference for compensating thermal drifts and non-specific adsorptions. Recently, we successfully demonstrated the MZI biosensor based on silicon oxides to directly detect the binding between biotin and streptavidin at the operating wavelength of 1,550 nm, the major telecom wavelength<sup>9</sup>. Silicon oxides have excellent optical properties, such as low absorption losses in visible and near infrared regions and easy fiber coupling, and their refractive index can be adjusted over a wide range between 1.45 (SiO<sub>2</sub>) and 1.90 (SiO) in the plasma enhanced chemical vapor deposition (PECVD) by changing reactant gases and relative flow rates.

C-reactive protein (CRP) is an important inflammation biomarker found in both vertebrates and invertebrates and a member of the pentraxin family of proteins. CRP is a homopentamer, which consists of five identical and non-covalently bound subunits assembled as a cyclic pentamer around a central pore<sup>10</sup>. CRP is produced by a liver and is normally present as a trace constituent of serum or plasma. The CRP biomarker is classified as an acute phase reactant in human and a significant marker of inflammation. Recent studies have proved the prognostic indicator in acute coronary syndromes and they also demonstrated the association between inflammation and cardiovascular disease (CVD)<sup>11-14</sup>. Inflammation is a major mechanism in the process of atherogenesis and in triggering of clinical CVD events. An elevated level of CRP represents a major risk factor in developing various forms of CVD like atherosclerosis, peripheral artery disease, myocardial infarction and strokes. High sensitivity CRP (hsCRP) based on enzyme linked immunosorbent assay (ELISA) is commonly used to determine

CRP in blood serum or plasma with a detection limit down to  $0.2 \,\mu g/m L^{15,16}$ . However, a false positive rate due to non-specific bindings and a principle of photometric detection may restrict the efficacy of the hsCRP ELISA. Moreover, matrices including saliva and lachrymal have been interested in the initial diagnostics of CRP levels, which requires more sensitivity and faster determination.

In this article, we demonstrated for the MZI biosensor to determine the binding of CRP to monoclonal anti-CRP. Its building block, a single-mode waveguide for total internal reflection, was designed by a finite element method (FEM) and then we suggested the guideline of microfabrication to achieve the singlemode waveguide. In addition, we introduced calixcrown self-assembled monolayers to guarantee an activity of capture proteins and to obtain a correct orientation of a monoclonal anti-CRP on the silicon oxides.

# **Results and Discussion**

#### **Basic Principle**

A main sensing principle is an integrated optic (IO) sensor effect in an optical waveguide, which was discovered by Lukosz and Tienfenthaler<sup>5</sup>. The optical waveguide defines as a material medium that confines and guides propagating electromagnetic waves. The IO sensor effect in the optical waveguide can be explained in terms of an effective refractive index (N) of the guided modes that are transverse electric  $(TE_m)$ and transverse magnetic (TM<sub>m</sub>) modes. The effective refractive index of each mode (N) depends on polarization (TE or TM), mode number m and wavelength  $\lambda$ , on the refractive index  $n_{core}$  and the dimensions of waveguide film and on the refractive indices of substrate and cover medium, n<sub>s</sub> and n<sub>c</sub>, respectively. If a material is surrounded by other materials with lower refractive indices, an incident light is confined and guided along the waveguide. However, a part of the guided wave called as an evanescent field penetrates a small distance  $\Delta z_c$  into a surrounding medium. The evanescent field decays exponentially proportional to

 $\exp\left(-\frac{z}{\Delta z_c}\right)$  with distance z from the waveguide surface. The penetration depth can be expressed as

race. The penetration deput can be expressed as

$$\Delta z_{\rm c} = \left(\frac{\lambda}{2\pi}\right) [N^2 - n_{\rm c}^2]^{1/2} \tag{1}$$

Thus, the IO sensor effect results from the interaction of the evanescent field with the surrounding environment. That is to say, the evanescent field is sensitive to the change in the refractive index distribution near the waveguide surface. This induces the change in the effective refractive indices of the guided modes ( $\Delta N$ ).

In immunosensor applications, the effective refractive index can be changed by two different effects. One is the formation of a functional layer due to the specific binding of antigen to antibody. This layer can be modeled as a homogenous layer F of thickness  $d_F$ and refractive index  $n_F$ . The other is the change in the refractive index of the homogeneous medium covering the waveguide surface. If both effects are simultaneously present, the change in the effective refractive index can be expressed as

$$\Delta N = \left(\frac{\partial N}{\partial d_F}\right) d_F + \left(\frac{\partial N}{\partial n_F}\right) n_F + \left(\frac{\partial N}{\partial n_c}\right) n_c$$
(2)

Interferometric detections are commonly used to convert a phase shift into an intensity variation that is directly measurable. We have chosen a Mach-Zehnder interferometer because of higher sensitivity and an internal reference for compensation of thermal drifts and non-specific adsorptions. In this configuration, an optical waveguide is split into two arms and after a certain distance L they recombine again. The waveguide is completely covered with a cladding layer and the only sensing zone is exposed to the outer medium in a certain area for the specific binding of antigen to antibody. The guided light in the sensing arm will experience a phase shift compared with that in the reference arm. Therefore, the interference of lights traveling through two arms causes the intensity modulation at the sensor output, which shows a sinusoidal variation related to effects described in Eq. (2). The oscillating relationship between the in-coupled intensity  $I_{\text{in}}$  and the out-coupled intensity  $I_{\text{out}}\xspace$  can be expressed as7,9,19

$$\frac{I_{out}}{I_{in}} \propto [1 + V\cos(\Delta \Phi + \Delta \Phi_o)]$$
(3)

where V, the visibility factor,  $\Delta \Phi$ , the phase shift between guided modes in the reference and sensor arm, and  $\Delta \Phi_0$ , an arbitrary relative phase due to possible inequalities of the optical path lengths of the two arms. The visibility factor V implies the contrast of the interference signal, the difference between maximum and minimum intensities. It also depends on the splitting ratios of the input and output Y-coupler and on the propagation losses of the guided mode in the interferometer arms. The phase shift  $\Delta \Phi$  can be given by<sup>7,9,19</sup>

$$\Phi = (\Phi_{\rm R} - \Phi_{\rm S}) = \frac{2\pi}{\lambda} L\Delta N \tag{4}$$

where L, the length of the sensor area,  $\lambda$ , the wavelength, and  $\Delta N$ , the change in the effective refractive index produced by the variation in the properties of the outer medium.

#### **Design and FEM Simulation**

A fundamental building block of the MZI immunosensor is an optical waveguide of total internal reflection (TIR), which implies the confinement of light in the material surrounded by other materials with lower refractive indices. A single-mode waveguide enables to develop the MZI sensor with performance and reproducibility. If the incident light with several modes is propagated via the waveguide, the optical intensity is divided among the modes and each mode will interact with the variations on the waveguide surface exposed to the outer medium. Because the conveyed information is liable to mutual interference and the fraction of power transferred from the light source to each mode is changed by the incident angle on the waveguide, the multi-mode waveguide is not suitable for robust biosensors. The rib waveguide is also considered to achieve a lateral confinement of light comparable to

the size of a single-mode optical fiber. We used the single-mode waveguide with a core thickness of a few micrometers at the operating wavelength of 1,550 nm, whilst other researchers have focused on the singlemode waveguide with a core thickness of hundreds of nanometers at the operating wavelength of 633 nm, which was achieved by the large difference between the refractive index of the core and cladding<sup>7,8,20,21</sup>. The different approach is related to the trade-off between surface sensitivity and insertion loss. In theory, the very thin core waveguide gives high surface sensitivity. However, the reduction of core dimensions for single mode behavior introduces disadvantages of mass production and large insertion losses when light is coupled with an optical fiber. Moreover, if the lossy substrate (e.g., Si and GaAs) is used for the MZI biosensor, thick cladding layers are required to reduce propagation losses. This can result in the longer fabrication process and the stress in a multilayered structure.

A numerical simulator based on a finite element

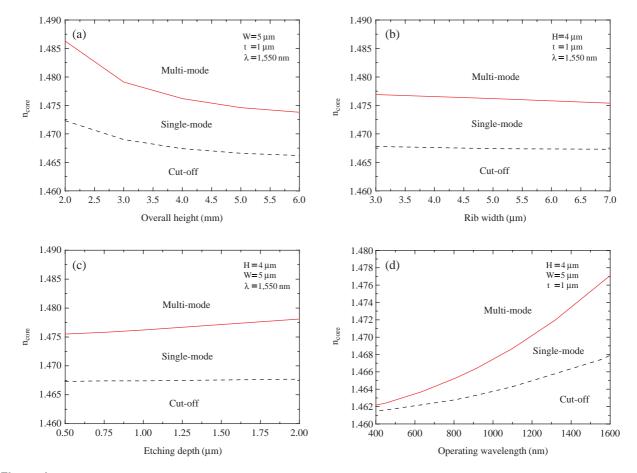


**Figure 1.** FEM simulation as a function of design parameters: (a) overall height (H), (b) rib width (W), (c) etching depth (t) and (d) operating wavength.

method was used to find the boundary between cutoff, single-mode and multi-mode regions. The singlemode behavior depends on the operating wavelength, the core thickness, the width and depth and the refractive index contrast between the core and the cladding layers. The simulation was set up using the waveguide structure illustrated in Figure 1, which a rib waveguide of silicon oxide ( $n_{core}$ ) on silica ( $n_s$ =1.458) and has an upper cladding that is PECVD SiO<sub>x</sub> ( $n_c$ =1.461). The simulations of mode analysis were repeated with different values of the core thickness (H), the width (W) and depth of the rib structure to find the boundaries, and the operating wavelength ( $\lambda$ ) for TM polarization. The criteria in mode analysis are expressed as

$$n_{core} > N_m > n_s, n_c (m=1, 2, 3, \cdots)$$
 (5)

where N<sub>m</sub> is the effective refractive index of the guided mode m. Figure 1 shows the modal behavior of the rib waveguides as design parameters. Both the refractive index of core and the permitted window for single-mode propagation increased as the decrease in the overall height, the decrease in width and the increase in the etching depth. The overall height had more significant effect on the refractive index of core and the permitted window than the width and the etching depth. The cut-off region below the broken line implies that TM waves cannot be guided and propagated via the rib waveguide. The effect of the operating wavelength on the refractive index of core is also illustrated in Figure 1. The refractive index of core and window for single-mode increased as the increase in the operating wavelength. It indicates that the longer waveguide is of great advantage in the viewpoint of the microfabrication. Furthermore, total attenuation in fused silica including Rayleigh scattering, impurity absorption and intrinsic absorption is minimized at  $\lambda = 1,550$  nm, which is commonly used for broadband communications (telecom and datacom)<sup>22</sup>. It means that the operating wavelength of 1,550 nm provides electronic data with high quality and low loss in a format that is readily analyzed and shared.

From these constructed maps related to design parameters, we are able to find the appropriate fabrication conditions for our purpose. However, a structure close to the transition condition of a mode has relatively high N and then the evanescent field penetrates into the sensing medium deeply. It is more sensitive to the change in the distribution of refractive index and so the better surface sensitivity can be achieved due to the higher index contrast. For the immunosensors with high sensitivity and performance, the operating wavelength and design parameters must be optimized in such a way that a large fraction of the guided mode travels through the sensing medium. Therefore, we have finally chosen the following rib structure at the operating wavelength of 1,550 nm for TM polarization: a silica substrate ( $n_s$ =1.458); a non-stoichiometric silicon oxide with the overall height of 4 µm; its refractive index between 1.4674 and 1.4762; the rib structure with the width of 5 µm and the etching depth of 1 µm; a PECVD SiO<sub>x</sub> with the thickness of 1.5 µm ( $n_c$  =1.461). Because fabrication parameters like overall height (H), width (W) and etching depth (D) depend entirely on the capabilities of our facilities.

#### The Efficacy of PECVD Silicon Oxides

The silicon oxides for the MZI biosensor are grown by plasma-enhanced chemical vapor deposition (PECVD), which is a special chemical vapor deposition process facilitated by a rf plasma, and it enables oxides to be deposited at relatively low temperature. The growth reaction of silicon oxides in PECVD is given by

$$SiH_{4(g)} + 2N_2O_{(g)} \rightarrow SiO_{2(s)} + 2N_{2(g)} + 2H_{2(g)}$$
 (6)

The refractive index of silicon oxides grown by PECVD can be varied with growth parameters including flow ratio  $R=[N_2O]/[SiH_4]$ , deposition temperature and rf power, and thus the flow ratio was changed to modulate the refractive index while both deposition temperature and RF power were kept constant. The incorporation of hydrogen and nitrogen into a matrix enables the film to have the refractive index ranging from 1.45 to 1.97. More recently, we reported that the nitrogen incorporation would affect surface heterogeneities including surface potential and polar component of surface energy<sup>23</sup>. Figure 2 shows the variation of the refractive index in SiO<sub>x</sub> films deposited at different

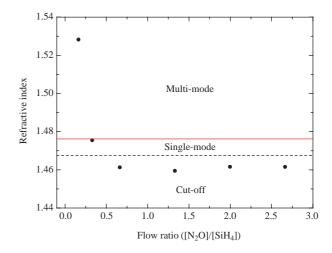


**Figure 2.** Refractive index of PECVD silicon oxides as a function of flow ratio  $R = [N_2O]/[SiH_4]$ .

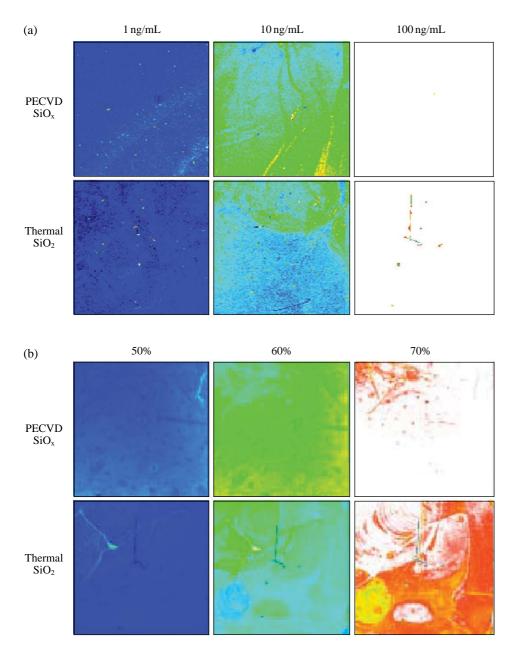


**Figure 3.** Rainbow color displays of PECVD silicon oxide selected as core material and thermally grown oxide as a function of (a) CRP concentration and (b) PMT gain.

flow ratios with mapping of achievable propagation modes. The refractive index decreased from a value about 1.53 down to 1.46 and then was saturated with the increase in the flow ratio. The high refractive index is due to silicon rich films. Therefore, we easily selected out the flow ratio of 0.34 for the PECVD deposition condition of the core silicon oxides and its refractive index was around 1.475 suitable for the singlemode propagation of our rib structure.

We also investigated an effect of a waveguide material on the immobilization of capture anti-CRP using fluorescence scanning analysis. Figure 3a shows the rainbow color display and fluorescence intensity of the selected silicon oxide and thermally grown oxide as a function of the concentration of CRP, respectively. The fluorescence intensity increased with the increase in the concentration of CRP and was saturated at the concentration of 100 ng/mL. The relative intensity of PECVD oxide was larger than that of thermal oxide. Clearly, when we decreased PMT gain at the saturation condition of 100 ng/mL, we could confirm the difference between PECVD and thermal oxides for the immobilization (Figure 3b). The increase in PMT gain improves sensitivity but also increases background noise and so it causes the saturation of fluorescence intensity. The fluorescence intensity decreased with the decrease in PMT gain. Importantly, the fluorescence intensity of PECVD oxide was larger than that of thermal oxide. We think that, even if the same protocol was used for the immobilization of capture anti-CRP, the selected PECVD oxide would be more effective on the protein immobilization than thermally grown oxide. The PECVD oxide may allow more activity of proteins captured on solid surface due to the correct orientation with high density and/or less conformational changes in the proteins.

It is known that the immobilization of capture Ab on the solid surface by Calixcrown-5 derivatives brings about the formation of a capture Ab monolayer in high density and the correct orientation to capture analyte proteins more efficiently than conventional immobilization processes, which allow random binding orientations<sup>17</sup>. ProLinker<sup>TM</sup> A, a calixcrown-5 derivative containing aldehyde groups, is the novel bi-functional molecular linker for efficient protein immobilization on the aminated surface. A coupling mechanism of proteins to ProLinker<sup>TM</sup> was proposed to be mediated by the ionized amine group of the capture proteins, which binds to the crown moiety of the linker molecule in a host-guest interaction. Hydrophobic interactions between hydrophobic residues of a protein and methoxy groups of the linker molecule are also involved in the protein immobilization. Therefore, we expected that the improved surface for the immobilization of capture proteins, to preserve their activity and maintain a correct orientation, would be very useful for the development of immunosensors with high sensitivity. We also observed that the PECVD oxide was more effective on the immobilization of capture anti-CRP than thermal oxide. According to the infrared absorption spectra of PECVD oxides<sup>9,23</sup>, PECVD oxides showed vibrations due to adsorbed water, Si-H stretching, N-H stretching, N-H ···· N stretching and SiO-H stretching, which were not observed in thermally grown oxide. We guess that these would affect the formation of calixcrown SAMs and/or the immobilization of capture anti-CRP. However, the verification of their effects takes us beyond the scope of this article. Moreover, the methods used for the immobilization of biological recognition species onto the surface of silicon oxides have been established well compared to other waveguide materials with high refractive index including Si<sub>3</sub>N<sub>4</sub>, TiO<sub>2</sub>, Ta<sub>2</sub>O<sub>5</sub> and LiNbO<sub>3</sub>. We are further exploring the efficacy of nitrogen-incorporated PECVD oxide on the protein immobilization.

#### Label Free Detection of C-reactive Protein

C-reactive protein (CRP) is an important inflamma-

tion biomarker found in both vertebrates and invertebrates and a member of the pentraxin family of proteins. It comprises five identical and non-covalently bound subunits assembled as a cyclic pentamer<sup>10</sup>. CRP is synthesized in the liver and is normally present as a trace constituent of serum or plasma. The CRP biomarker is classified as an acute phase reactant in human and a marker of inflammation with a half-life of ~19 h. Recent studies have demonstrated the association between inflammation and cardiovascular disease (CVD)<sup>11-14</sup>. An elevated level of CRP represents a major risk factor in developing various forms of CVD like atherosclerosis, peripheral artery disease, myocardial infarction and strokes. Nowadays, an enzyme-linked immunosorbent assay (ELISA) is the most common immunosensor which involves in optical detection. This is well established and shows sufficient sensitivity and reproducibility for CRP in serum or plasma. However, the conventional ELISA shows a relatively high false positive rate due to nonspecific bindings and it is also influenced by the color of the medium and its composition because of the photometric detection principle. In addition, the typical ELISA needs the incubation time of approximately 5 hours and the matrices, such as saliva and lachrymal, has been much interested in the initial stage of determining CRP levels. We believe that a new immunosensor with high sensitivity and quick speed for measurement and analysis is strongly on demand for the diagnostic, clinical and epidemiological applications.

Our MZI immunosensors with an interaction length of 500  $\mu$ m was tested to evaluate the feasility of the label free detection of CRP with high sensitivity. The capture anti-CRP (50  $\mu$ g/mL) was immobilized onto the sensor surface to bind the CRPs by the formation of calixcrown SAMs. Figure 4 shows normalized output signals for the binding of CRP to monoclonal anti-CRP as a fuction of CRP concentration. The normalized output signal increased with the increase in the CRP concentration. Our MZI immunosensor based on PECVD silicon oxides retained the ability to detect CRP even at a low concentration of 1 ng/mL. We expect that the detection limit would be less than the concentration of 1 ng CRP per mL. The refractive index of protein solutions measured by an Abbe refractometer and the effective refractive index obtained by the MZI sensor with various concentrations are listed in Table 1. We emphasize that the binding of antigen to antibody would cause the change in the refractive index and thickness of functional layers at the sensing zone because the refractive index of outer medium was not changed much to affect the effective index of the guided light. Among evanescent wave techniques, a surface plasmon resonance (SPR) biosensor has been

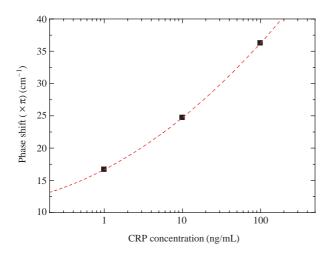


**Figure 4.** Normalized output signal as a function of CRP concentration.

**Table 1.** Refractive indices of antigen PBS solutions and effective refractive indices as a function of CRP concentration.

CRP concentration (ng/mL)	1	10	100
Refractive index	1.3331	1.3330	1.3328
Effective refractive index	1.46963	1.47088	1.47267

applied to recognize and detect the binding of CRP to anti-CRP. For instance, Hu et al.24 reported that the detection limit of the SPR bioassay for pCRP nto Mab C8 could reach 1  $\mu$ g/mL or even less. Meyer *et al.*<sup>25</sup> found a linear detection range of 2-5 µg CRP per mL on biotinylated antiCRP C6 using SPR. On the other hand, a dual polarization interferometric biosensor has been used to study the interaction kinetics between a monoclonal anti-CRP IgG and homopentameric CRP<sup>26</sup>. Except optical transduction mechanisms, a few researchers have been interested in the label-free CRP detection using other sensing mechanism. Aizawa et al.<sup>27</sup> constructed an immunosensor system to combine a quartz crystal microbalance with the agglutination reaction of immunized latex beads for CRP detection in serum. Micromachined cantilevers based on the resonant frequency shift and the piezoresistive response were introduced to detect CRP without any labeling and optical measurement<sup>28,29</sup>. The piezoresistive selfsensing microcantilever on monoclonal anti-CRP immobilized using calixcrown (ProLinker<sup>TM</sup> B, Proteogen, Korea) SAMs on Au surface has detected the CRP at the concentration of 100 ng/mL. Recently, Meyer et al.<sup>30</sup> reported a new technique (called frequency mixing) for detecting CRP levels in various matrices. They used a two-frequency magnetic field

excitation and detected the magnetic response at a third frequency which was a linear combination of the applied frequencies. They showed that the linear detection window was ranging from 25.0 ng/mL to 2.5  $\mu$ g/mL.

# Conclusions

To monitor and diagnose diseases, the quantitative detection of biomarker proteins, which is directly relevant to various diseases, is required and so it allows us to precisely diagnose given disease by the detection of appropriate protein. In this article, we have developed the Mach-Zehnder interferometer (MZI) sensor based on PECVD silicon oxides for the labelfree detection of C-reactive protein (CRP), and the refractive index of the waveguide core was accurately controlled by changing the flow ratio  $[N_2O]/[SiH_4]$  to achieve the single-mode behavior of large core waveguides combined with a finite element method. We has used the binding of CRP to monoclonal anti-CRP as a model binding reaction and successfully demonstrated that our MZI sensor had the detection limit of 1 ng/mL or even less at the operating wavelength of 1,550 nm. Although more systematic biological studies are necessary to verify the efficacy of our MZI immunosensor, we believe that the MZI immunosensor is a very promising candidate of biomarker detections with no labeling, high sensitivity, quick speed and free choice of sample matrix and origin. Besides the immunosensor applications, this MZI configuration can be adopted for academic researchers to explore and understand the affinity and kinetics of a biological reaction and the structureal changes taking place in biomolecules as environmental factors like pH, salt, temperature, solvents and buffers. On the cutting edge of drug discovery, high throughput screening (HTS) has been required to identify pharmacologically active compounds and optimize the biological activity of a lead compound rapidly. It may also be a promising candidate to accelerate the developments of HTS techniques and to utilize efficiently combinatorial chemistry techniques. Moreover, it has attractive features for lab-on-a-chip devices functioning as portable or hand held personal laboratories, a potential of pointuse detection of clinical or environmental parameters without any labeling. However, a light source, a detector and related optical components should be monolithically integrated with microfluidic platforms for developing high throughput analytical nano/microsystems. Other than monolithic solutions to integration like external mounting, hybrid integration and complicate packaging, require high precision alignment

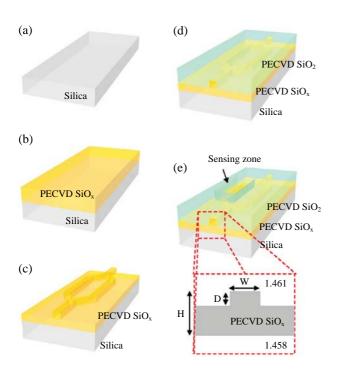


**Figure 5.** Microfabrication procedures of Mach-Zehnder immunosensors.

and become impractical and costly. If monolithic integration technology with optical self-alignment features is available, lab-on-a-chip and high throughput system concepts can materialize to fully exploit the advantages of integrated optics in an inexpensive way. Equally, the nano/microfluidic platforms will give various advantages including a reduced mixing time, a fast response, small volumes and compact sensing system.

# **Materials and Methods**

#### **Microfabrication Procedures**

Figure 5 illustrates the microfabrication process of a Mach-Zehnder interferometer based on silicon oxides. The silica wafer (Ewafer Co., Korea) was cleaned to remove organic residues with piranha solution (H<sub>2</sub>SO<sub>4</sub> : H<sub>2</sub>O<sub>2</sub>=3 : 1) for 10 min. It was then rinsed in deionized (DI) water and dried with hot nitrogen gas using a spin rinse dryer. Also, it was baked to dehydrate at 200°C for 10 min on a hot plate. The non-stoichiometric silicon oxide as a waveguide core was deposited on the substrate at 250°C in a parallel-plate type Plasma Thermo 790 PECVD reactor. The refractive index of the core layer could be modulated with the ratio of oxygen to silicon. The flow ratio of nitrous oxide (N<sub>2</sub>O) gas to silane (2% SiH<sub>4</sub>/H<sub>2</sub>) gas was varied to adjust the refractive index for single-mode waveguide. Rib

waveguides for optical confinement were defined using a photolithographic technique. The wafer was coated with the AZ P4620 photoresist (Clariant, Muttenz, Switzerland using a spin coater at 3,000 rpm for 40 sec, and then it was baked on a hot plate at 95°C for 2 min. The i-line (365 nm) exposure was used for photolithography using a mask aligner (Karl Suss MA6, SUSS MicroTech, Germany) with an expose dose of 17 mW/cm<sup>2</sup>. The photoresist was developed by immersing the exposed substrate in a developing solution (AZ300MIF, Clariant, Muttenz, Switzerland). The resulting patterns were then hard-baked to harden the unexposed PR at 110°C for 2 min on a hot plate. The patterns were transferred into the core layer using reactive ion etching (RIE). The upper cladding of silicon oxide was deposited on the patterned core layer using the same PECVD reactor. A sensing zone was opened in one of the interferometer arms using RIE. Finally, the wafer was cut into an individual chip using an automatic dicing system and then the sides for input and output were mechanically polished for end-fire coupling.

#### **Optical Characterization**

The optical characterization was performed with transverse magnetic (TM) wave from a stabilized laser diode. The operating wavelength was the major telecom wavelength of 1,550 nm. The light was coupled into the waveguide through a single-mode fiber (SMF) with a mode-field diameter of 9 µm. The optical fiber was placed in straight line to preserve the input TM-polarization, and the end of SMF was placed in front of the waveguide core to couple light into the MZI (end-fire coupling). Light was collected by a multi-mode fiber connected to an optical powermeter (ML9001A, Anritsu Co., Japan). The intensity of output light was monitored by homemade software and data acquisition hardware (USB-6009, National Instruments Co., USA). Precise translation stages were used for the accurate alignment of all the components with a zoom stereo microscope and accessories (SZ-51 series, Olympus Co., Japan). Alternatively, a microscope objective  $(40 \times)$  and an IR vidicon camera were used to record the near-field pattern at the end of the MZI that showed the modal behavior of the fabricated waveguide.

The refractive index of non-stoichiometric silicon oxides was measured by a prism coupler (Model 2010, Metricon Co., USA). The prism coupler treats the film to be measured as an optical waveguide and so the observed mode angles enable us to calculate film thickness and refractive index. It is superior to the ellipsometer for measuring typical thick films of non-stoichiometric dielectric materials, photoresists or polymeric films. The films are contact with the base of a prism, which is operating pneumatically, while creating a small air gap between the film and the prism. A laser beam strikes the base of the prism and is normally reflected onto a photodetector. However, at certain discrete values of the incident angle, the light enters into the films and so this causes a sharp drop in the intensity of light. From the intensity of reflected light versus the angle of incidence, both refractive index and film thickness can be calculated with the assistance of the Model 2010 data analysis software.

# SAMs Formation and Monoclonal Anti-CRP Immobilization

After the microfabrication, the interferometer have to be functionalized to determine the antigen (Ag)-antibody (Ab) interaction at its surface by a thin layer that exposes the selected binding sites to the complementary analyte in the aqueous solution. Thus, we introduce a novel immobilization method to capture proteins, which uses a calixcrown derivative (ProLinker<sup>TM</sup> A, Proteogen, Korea) with bi-functional cross liking properties containing aldehyde (-CHO) groups for the formation of a self-assembled monolayer on aminated glass substrates and a crown moiety that provides a molecular recognition site for protein immobilization. It provides a simple process and effective high density protein immobilization without an activity loss or incorrect orientation of the capture protein<sup>17</sup>. First of all, the surface of the MZI sensor was functionalized using silanization procedures<sup>18</sup> using N-[3-(trimethoxysilyl)propyl]-ethylene diamine (Sigma-Aldrich, UK) to provide free amine at the sensor surface. The sensor chip was cleaned with acetone and blown dry with nitrogen gas. It was immersed in anhydrous ethanol containing 1% N-[3-(trimethoxysilyl)propyl]-ethylene diamine for 20 min. Then it was rinsed with ethanol and DI water and dried. The formation of calixcrown self-assembled monolayers (SAMs) was accomplished by immersing the aminated MZI in CHCl<sub>3</sub> solution containing 10 mM Calix[4] arene-crown-5 for 5 hours. It was rinsed with CHCl<sub>3</sub> solution and acetone, and then dried. The calixcrown SAMs have the special properties in protein immobilization that the crown moiety of the linker molecule binds the ionized amine group of proteins and the methoxy groups of the linker molecule interact with the hydrophobic residues of a protein<sup>17</sup>. Monoclonal anti-CRP (Scripps laboratories Inc., San Diego, CA, USA) was dissolved in phosphate buffered saline (PBS, pH 7.4) and incubated on the Calixcrown SAMs for 1 hour. Then the sensor was rinsed with PBS and dried. Blocking was performed using bovine serum albumin (Sigma, St. Louis, MO, USA) in order to prevent nonspecific bindings on the sensor surface for 1 hour.

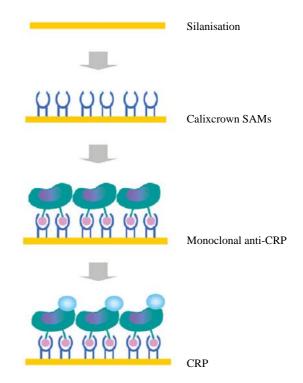


**Figure 6.** Schematic diagram of monoclonal anti-CRP immobilization using Calixcrown SAMs on the aminated silicon oxides.

Finally, the MZI was washed out with PBS and dried with nitrogen gas for 1 min. For quantitative analysis of the MZI sensor, one  $\mu$ L of CRP antigen was diluted with PBS solution in three different concentrations (1 ng/mL, 10 ng/mL and 100 ng/mL). Figure 6 illustrates a schematic diagram of SAMs formation and monoclonal anti-CRP immobilization.

To confirm specific binding after the Ag-Ab interaction and investigate an effect of a waveguide material on a capture protein immobilization, CRP antigen-antibody binding experiments on PECVD silicon oxides and thermally grown SiO<sub>2</sub> were conducted using Cy5 (Amersham Biosciences, Piscataway, NJ, USA) fluorescence labeled CRP (Scripps laboratories Inc., San Diego, CA, USA). The immobilized surface was immersed into Cy5 labeled CRP antigen solution and then incubated at 37°C for 1 hour in a humidity chamber. The MZI was washed out with PBS containing polyoxyethylenesorbitan monolaurate (Tween 20, St. Louis, MO, USA) and dried with nitrogen gas. Then, the protein immobilization and Ag-Ab interaction were investigated using a fluorescence scanner (Scan-Array<sup>™</sup> Lite, GSI Lumonics, Kanata, Ontario, Canada) with a ScanArray<sup>TM</sup> Express software. The scanner was set to optimize the quality of fluorescence images by adjusting the laser power and photomultiplier tube (PMT) gain. The fluorescence intensity of each sample was determined and displayed as both colored images and relative numerical values.

# Acknowledgements

We thank Ho Min Byun and Gil Sun No at the Micro-Nano Fabrication Center of the Korea Institute of Science and Technology (KIST) for helps about microfabrication including PECVD and RIE. This work was supported by the Ministry of Science and Technology ("Protein Chip Technology Research Center" and "21C Frontier R & D Program"). J. Hong was partially supported by the Korea Research Foundation Grant funded by the Korean Government (MOEHRD) (KRF-2006-214-D00056).

# References

- Luppa, P.B., Sokoll, L.J. & Chan, D.W. Immunosensors-principles and applications to clinical chemistry. *Clinica Chimica Acta* 314, 1-26 (2001).
- 2. Paek, S.-H. *et al.* Immunosensors for point-of-care testing. *Biochip Journal* **1**, 1-16 (2007).
- Shankaran, D.R., Gobi, K.V.A. & Miura, N. Recent advancements in surface plasmon resonance immunosensors for detection of small molecules of biomedical, food and environmental interest. *Sensors and Actuators B-Chemical* **121**, 158-171 (2007).
- Hong, N.K. *et al.* Label-free detection of antibodyantigen interaction by Si nanowire MOSFET. *Biochip Journal* 2, 255-260 (2008).
- Tiefenthaler, K. & Lukosz, W. Sensitivity of grating couplers as integrated-optical chemical sensors. J. Opt. Soc. Am. B 6, 209-220 (1989).
- Optical Sensors: Industrial Environmental and Diagnostic Applications, ed. R. Narayanaswamy, O.S. Wolfbeis, Springer, 1st edition (2004).
- 7. Prieto, F. *et al.* An integrated optical interferometric nanodevice on silicon technology for biosensor applications. *Nanotechnology* **14**, 907-912 (2003).
- Ymeti, A. *et al.* Integration of microfluidics with a four-channel integrated optical Young interferometer immunosensor. *Biosensors and Bioelectronics* 20, 1417-1421 (2005).
- Hong, J. *et al.* A Mach-Zehnder interferometer based on silicon oxides for biosensor applications. *Analytica Chimica Acta* 573-574, 97-103 (2006).
- Motie, M., Brockmeier, S. & Potempa, L.A. Binding of model soluble immune complexes to modified Creactive protein. *J. Immunol.* 156, 4435-4441 (1996).
- Ferranti, S. & Rifai, N. C-reactive protein and cardiovascular disease: a review of risk prediction and interventions. *Clinica Chimica Acta* 317, 1-15 (2002).
- 12. Mazer, S.P. & Rabbani, L.E. Evidence for C-reactive

protein's role in (CRP) vascular disease: atherothrombosis, immune-regulation and CRP. *J. Thromb. Thrombolysis* **17**, 95-105 (2004).

- Li, J.J. & Fang, C.H. C-reactive protein is not only an inflammatory marker but also a direct cause of cardiovascular diseases. *Med. Hypoth.* 62, 499-506 (2004).
- Lloyd-Jones, D.M., Liu, K., Tian, L. & Greenland, P. Narrative review: assessment of C-reactive protein in risk prediction for cardiovascular disease. *Annals of Internal Medicine* 145, 35-42 (2006).
- Dominici, R., Luraschi, P. & Franzini, C. Measurement of C-reactive protein: two high sensitivity methods compared. J. Clin. Lab. Anal. 18, 280-284 (2004).
- Clarke, J.L. *et al.* Comparison of differing C-reactive protein assay methods and their impact on cardiovascular risk assessment. *Am. J. Cardiol.* 1, 155-158 (2005).
- Lee, Y. *et al.* ProteoChip: a highly sensitive protein microarray prepared by a novel method of protein, immobilization for application of protein-protein interaction studies. *Proteomics* 3, 2289-2304 (2003).
- Immobilized Biomolecules in Analysis: A Practical Approach, ed. T. Cass and F.S. Ligler, Oxford University Press, New York (1998).
- Maisenholder, B. *et al.* A GaAs/AlGaAs-based refractometer platform for integrated optical sensing applications. *Sensors and Actuators B* 39, 324-329 (1997).
- 20. Qi, Z.M. *et al.* A design for improving the sensitivity of a Mach-Zehnder interferometer to chemical and biological measurands. *Sensors and Actuators B* **81**, 254-258 (2002).
- Hua, P. *et al.* Integrated optical dual Mach-Zehnder interferometer sensor. *Sensors and Actuators B* 87, 250-257 (2002).
- Clifford, R.P. "Fundamentals of Optoelectronics", Richard, D., Irwin, Inc. 1995, ch. 7, pp. 175-185.
- 23. Hong, J. *et al.* The effect of nitrogen incorporation on surface properties of silicon oxynitride films. *Phys. Status Solidi RRL* **3**, 25-27 (2009).
- Hu, W.P. *et al.* Immunodetection of pentamer and modified C-reactive protein using surface resonance biosensing. *Biosensors and Bioelectronics* 21, 1631-1637 (2006).
- 25. Meyer, M.H.F., Hartmann, M. & Keusgen, M. SPRbased immunosensor for the CRP detection a new method to detect a well known protein. *Biosensors* and *Bioelectronics* 21, 1987-1990 (2006).
- Lin, S.M. *et al.* Homopolyvalent antibody-antigen interaction kinetic studies with use of a dual-polarization interferometric biosensor. *Biosensors and Bioelectronics* 22, 715-721 (2006).
- Aizawa, H. *et al.* Conventional diagnosisof C-reactive protein in serum using latex piezoelectric immunoassay. *Sensors and Actuators B* 76, 173-176 (2001).
- Lee, J.H. Label free novel electrical detection using micromachined PZT monolithic thin film cantilever for the detection of C-reactive protein. *Biosensors and Bioelectronics* 20, 269-275 (2004).
- 29. Wee, K.W. et al. Novel electrical detection of label-

free disease marker proteins using piezoresistive selfsensing micro-cantilevers. *Biosensors and Bioelectronics* **20**, 1932-1938 (2005).  Meyer, M.H.F. CRP determination based on a novel magnetic biosensor. *Biosensors and Bioelectronics* 22, 973-979 (2007).